Development and Test of an Integrated Sensory System for Advanced Aircraft

W.K. Toolan* and A.M. Zislin†
Grumman Aerospace Corporation, Bethpage, New York

This paper presents the results of the second phase of an integrated sensory subsystem (ISS) development effort. The ISS is a combination of redundant inertial sensors, air data probes, transducers, other flight control related sensors, interfaces, and the associated data handling system (DHS). The sensor data derived within the ISS meets the requirements (performance, redundancy, survivability, etc.) for digital fly-by-wire flight control systems. The key task of this development phase was the synthesis and development of a DHS for dispersed arrays of flight control inertial sensors subjected to dissimilar motions due to body bending of the aircraft structure. The system design is described in terms of the hardware and data handling system synthesis, followed by a discussion of the methods and results utilized to verify the system design.

Nomenclature

a_B = accelerations due to bending
a_k = accelerations in laboratory simulation
C = noise influence matrix
$E\{\ \}$ = expectation operator
G = steady-state Kalman weighting matrix
h = distance of sensors to c.g.
ℓ = distance of sensors to modal reference point
Kop = thousands of operating per second
M = measurement matrix
P = covariance matrix
p = aircraft roll rate
q = aircraft pitch rate
r = aircraft yaw rate
Δt = sample time of discrete system
$u_k, \dot{u}_k$ = discrete control position and rate command
x_k = discrete state vector
x^e_{k+1} = extrapolated state vector
$\hat{x}_{k+1}$ = estimated value of state vector
y_k = discrete measurement vector
$\Gamma_1(\Delta t)$ = control position influence matrix
$\Gamma_2(\Delta t)$ = control rate influence matrix
ϵ_k = discrete estimation error or residual
η_k = system noise
ν_k = measurement noise
$\xi, \dot{\xi}, \ddot{\xi}$ = displacement, rate, acceleration of generalized structural coordinates
$\Phi(\Delta t)$ = discrete state transition matrix
Φ_m = mode shape matrix
Ψ_m = mode slope matrix
ω_B = rotational rates due to bending
ω_R = rigid body rotational rates
ω_T = flight attitude table rates
$\omega^e_{B_{k+1}}$ = extrapolated structural bending rates

Symbols

$(\hat{\ })$ = estimated quantity
$(\dot{\ })$ = derivative
$\times$ = vector cross product

Superscript

e = extrapolated quantity

Subscripts

B = bending quantity
$k, k+1$ = sample times
NORM = normalized quantity
R = rigid quantity

Received Nov. 12, 1981; revision received Jan. 7, 1982.

*Senior Engineer.
†Senior Engineer. Member AIAA.

Introduction

FUTURE aircraft design philosophy that incorporates relaxed static stability imposes increased demands for redundancy, reliability, and survivability on the aircraft's flight control system. In order to meet these demands, while minimizing hardware proliferation, a new aircraft sensor configuration and data handling system (DHS) concept was developed. The integrated sensory subsystem (ISS) attacks the problem of sensor proliferation by minimizing the quantity of each sensor type while maximizing the number of user systems in a manner that is consistent with the performance, reliability, redundancy, and survivability requirements. The ISS achieves these goals with design techniques that maximize the use of mature sensor technology, modularization, interchangeability, and the capability of self-contained fault detection and isolation. These techniques utilized dispersed sensor configurations to enhance system survivability and maintainability.

The first element of the ISS is a sensor set consisting of hard-mounted, skewed, and dispersed rate integrating gyros and accelerometers; low- and high-speed air data probes located in close proximity to modularized air data transducers; an inertial navigation system (INS), pilot command sensors, surface position sensors, radio navigation devices, terminal guidance sensors, and landing aids. The ISS concept is shown in Fig. 1.

The second element is a reliable and survivable input/output (I/O) bus that links the sensory data to three or more flight control computers.

The last major element of the ISS is a computation network within the redundant computer complex consisting of the system software. This software performs several tasks, including sensor signal selection through failure detection and isolation algorithms, state estimation and sensor data normalization algorithms to account for the effects of deterministic errors associated with the dispersed sensors and random sensor noise, strapdown attitude and heading computations, and air data computations.

The ISS-I Feasibility and Design Study reported by Weinstein, Abrams et al.[1-4] provided the framework for a multiphase development effort in which various portions of the ISS system could be developed. These include:

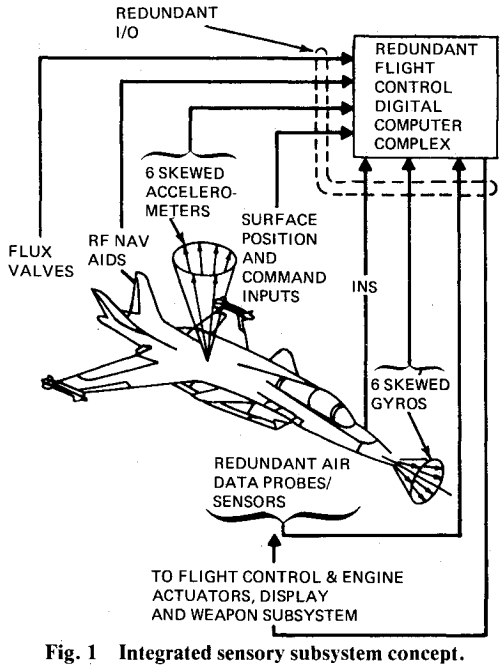

Fig. 1 Integrated sensory subsystem concept.

1) Development of a dispersed/redundant array of accelerometers and DHS for flight control stabilization applications.

2) Development of a dispersed inertial component and DHS for both flight control and attitude heading reference applications.

3) Development of a dispersed/redundant air data system for conventional takeoff and landing aircraft.

4) Development of an air data system for the low-speed regime (i.e. <60 knots).

5) Development of a low-cost navigation system utilizing complementary filters to mix inertial, air data, magnetic heading, and radio/landing aid data.

This paper presents the results of the first of the above development efforts, i.e., development and laboratory test of a DHS for a dispersed array of flight control gyros and accelerometers.

System Synthesis

ISS Inertial Sensor Configuration

The six gyros and six accelerometers of the ISS are dispersed to assure a survivable system. Although the sensors are dispersed, their input axes are skewed to effectively form the cones shown in Fig. 1. The cone axis for the gyros lies along the aircraft longitudinal axis and the accelerometer cone axis lies along the yaw axis. This conical array with associated DHS provides a two-fail operational capability. Orientation of the cone axes and selection of cone angles is based upon the maximum sensor reading anticipated in each axis and the axis about which the maximum level typically occurs. Details of this selection process are given in Ref. 5.

Data Handling System

Data from the skewed gyros and accelerometers are processed in redundant computers by the ISS DHS. The DHS consists of gyro and accelerometer redundancy data management (RDM) routines and a state estimator that is used to normalize the raw sensor data. The DHS configuration is shown in Fig. 2.

The RDM for the gyros and the accelerometers consists of the three major elements depicted in Fig. 3: transient failure removal, voting computational, and failure isolation routines. The transient failure removal routine applies a rate of change reasonableness criteria to the individual sensor readings and removes any sensor that fails the criteria from the voting logic. A sensor that subsequently passes the reasonableness

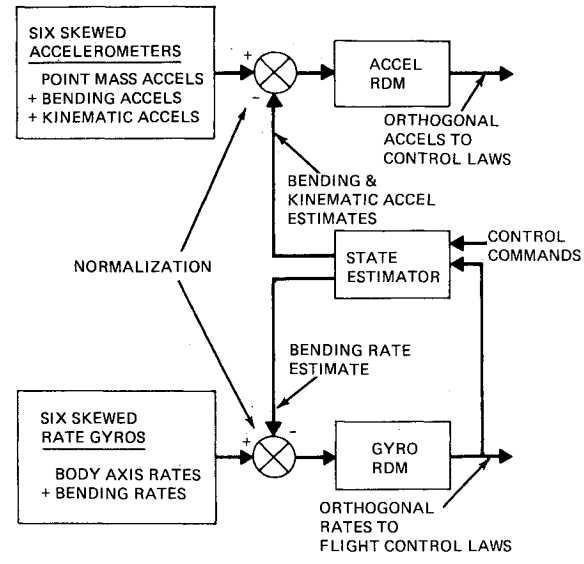

Fig. 2 ISS data handling system.

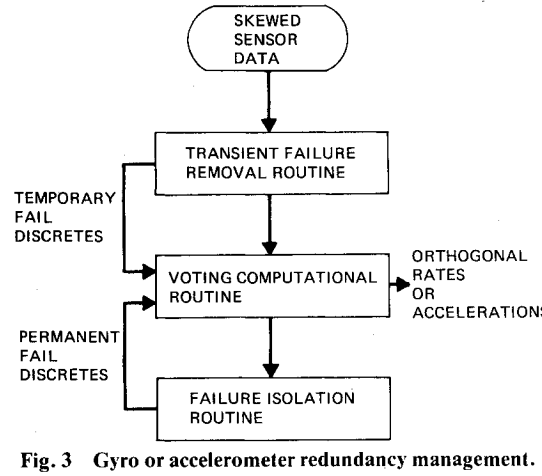

Fig. 3 Gyro or accelerometer redundancy management.

criteria is reinstated as a candidate in the voting routine. The voting computational routine selects the best of the sensors which have not been declared temporarily or permanently failed and computes the orthogonal output data. The selection process for this routine is based upon a least squares best estimate of the error for each sensor. The failure isolation routine applies scale factor error/bias level criteria to each active sensor. If a sensor exceeds the failure threshold level for a sufficient number of iterations that sensor is declared a permanent failure and is removed from further consideration by the RDM.

The accelerometer and the gyro RDMs utilize similar logic for their respective transient failure, voting, and failure isolation routines. The major differences between them are in the input axes cone angle and orientation and the failure monitoring thresholds. It is to be noted that failure monitoring thresholds and time delays for the RDMs are selected for the specific characteristics of the sensors, the aircraft, and the flight control system used for a particular application. The criteria and rationale for the threshold selection process are given in Ref. 1.

The state estimator used in the DHS is required to compensate for structural bending effects and kinematic acceleration effects.

Structural bending of an aircraft in flight can potentially cause two difficulties with skewed and dispersed body-mounted gyros and accelerometers. The first problem results from the difference in bending and kinematic effects that are sensed by the various sensors. These differences make it

difficult to effectively compare sensor data in a sensor redundancy management scheme. The second problem that can arise from dispersion of flight control system sensors is a structural mode coupling through the sensors with the control system, resulting in unsatisfactory or unstable control system performance.

In order to preclude problems resulting from structural bending and kinematic effects a state estimator was developed to generate estimates of these effects; these estimates are used to normalize sensor data prior to performing sensor RDM.

The effect of the structural bending on the body mounted accelerometers can be represented as

$$a_B = \Phi_m \ddot{\xi} + \dot{\omega}_B \times \ell \tag{1}$$

where $\Phi_m \ddot{\xi}$ are the linear accelerations caused by sensor translation during flexing, and $\dot{\omega}_B \times \ell$ are the linear accelerations caused by sensor rotation during flexing.

The bending effect on the gyros is represented by

$$\omega_B = \Psi_m \dot{\xi} \tag{2}$$

where $\Psi_m \dot{\xi}$ are the angular rates caused by sensor rotation during flexing.

In addition to bending effects, the off c.g. mounted accelerometers will sense linear acceleration due to the effect of aircraft rotations. The total sensed accelerations and rates are expressed as the sum of the rigid-body motions and the bending motions,

$$a_T = \sum \frac{F_{\text{APPLIED}}}{\text{MASS}} + \Phi_m \ddot{\xi} + (\dot{\omega}_B \times \ell) + (\dot{\omega}_R \times h) + \omega_R \times (\omega_R \times h) \tag{3}$$

$$\omega_T = \omega_R + \Psi \dot{\xi} \tag{4}$$

The effect of sensor dispersion is accounted for in Eqs. (3) and (4) by using the appropriate mode shapes (Φ_m), mode slopes (Ψ_m), and displacements (ℓ and h) for each sensor. The state estimator generates estimates of $\dot{\xi}$, $\ddot{\xi}$, and ω_R so that the bending and kinematic effects in Eqs. (3) and (4) can be calculated.

For this study, the structural flexibility effect taken into account in the state estimator are the four bending modes given in Table 1. A simplify assumption made for this design is that the symmetric and antisymmetric modes are decoupled and that these coupling effects are lumped into the system noise N_K.

In the longitudinal portion of the state estimator, the flexible modes are excited by control system inputs and aerodynamic coupling. For the lateral-directional portion of the state estimator, it was assumed that the aero coupling was negligible.

The state estimator is derived by minimizing the error, ϵ_{k+1} between the true and estimated state which, in turn, minimizes the covariance matrix

$$P_k = E\{(x_{k+1} - \hat{x}_{k+1})(x_{k+1} - \hat{x}_{k+1})^T\} \tag{5}$$

where $\epsilon_{k+1} = x_{k+1} - \hat{x}_{k+1}$ is the estimation error.

In discrete form, the aircraft equations of motion can be written in vector form as

$$x_{k+1} = \Phi(\Delta t) x_k + \Gamma_1 u_k + \Gamma_2 \dot{u}_k + C\eta_k \tag{6}$$

with measurements

$$y_{k+1} = M x_{k+1} + \nu_{k+1} \tag{7}$$

The estimator update equation is written as

$$\hat{x}_{k+1} = x^e_{k+1} + G(y_{k+1} - M x^e_{k+1}) \tag{8}$$

where the extrapolated state is

$$x^e_{k+1} = \Phi(\Delta t)\hat{x}_k + \Gamma_1 u_k + \Gamma_2 \dot{u}_k \tag{9}$$

Since $G = f(P_K)$, minimizing P_K gives the optimum value of G, the steady-state estimator weighting matrix (see Ref. 6).

The estimator design for the flight control application discussed in this paper consists of 8 longitudinal states and 11 lateral directional states. The estimator is implemented in a straightforward manner with the only inputs being the control commands and the normalized rate data as shown in Fig. 2.

The first step in each iteration is to extrapolate the previous state estimate via Eq. (9). The structural and kinematic portions of the rate and acceleration signals can then be formed as the extrapolated quantities,

$$\Psi \dot{\xi}^e_{k+1}, \Phi \ddot{\xi}^e_{k+1} \quad \text{and} \quad \dot{\omega}^e_R \times h \tag{10}$$

These terms are transformed into the skewed coordinate system and subtracted from the sensed data,

$$\omega_{\text{NORM}_{k+1}} = \omega_{\text{SENSED}} - \Psi_m \dot{\xi}^e_{k+1} \tag{11}$$

$$a_{\text{NORM}} = a_{\text{SENSED}} - \Phi_m \ddot{\xi}^e_{k+1} - (\dot{\omega}^e_{B_{k+1}} \times \ell) - (\dot{\omega}^e_R \times h) \tag{12}$$

where

$$\dot{\omega}^e_{B_{k+1}} = \Psi_m \ddot{\xi}^e_{k+1}$$

The normalized signals are then fed to the RDM where failure detection and isolation occur and a set of orthogonal rate and acceleration values is generated. The extrapolation error is computed as

$$\epsilon_{k+1} = \begin{bmatrix} p_{\text{NORM}} - p^e_{k+1} \\ q_{\text{NORM}} - q^e_{k+1} \\ r_{\text{NORM}} - r^e_{k+1} \end{bmatrix} \tag{13}$$

and the new estimate of the state vector is formed as in Eq. (8),

$$\hat{x}_{k+1} = x^e_{k+1} + G\epsilon_{k+1} \tag{14}$$

The system is then ready for the next iteration. The iteration rate used for sensor processing, the state estimator and the flight control laws in this design is 10 samples/s. Refer to Ref. 7 for a discussion of sample rate selection.

It is to be noted that the state estimator design described above does not reduce the need for high-frequency analog prefilters; these must be included in the computer I/O to minimize the aliasing of high-frequency noise and bending.

Table 1 Bending modes used in ISS study

Mode	Model frequency, Hz	Damping	Generalized mass, slugs-ℓ^2
1) 1st fuselage vertical bending	7.62	0.019	51.5
2) 1st wing symmetric bending	4.4	0.016	7.21
3) Fuselage lateral bending	8.98	0.035	15.1
4) 1st wing anti-symmetric bending	5.36	0.027	9.0

The DHS described above, when programming in efficient assembly language, requires 30K of memory and can be executed in 20 ms in a 200 Kop machine.

Digital Simulation

The gyro/accelerometer DHS discussed previously was integrated into an existing six degree-of-freedom (DOF) simulation of the F-14, as shown in Fig. 4. This integrated F-14/ISS simulation program was used to perform ISS systems evaluation. The program simulates various aircraft trajectories which are generated by applying input commands (i.e., stick or pedal motions) to the digital flight control laws which were developed in a previous study.[7] Initially, the aircraft is statically trimmed at a specified Mach number and altitude for level flight. Following the trim iteration, the equations of motion, control equations, and steering are solved and integrated by the Runge-Kutta numerical integration method. The aircraft parameters are generated throughout the trajectory at the desired iteration rate. The switch shown in Fig. 4 represents a software option to select either open- or closed-loop evaluations. In the open-loop configuration, the digital flight control laws receive the required rates and accelerations from the F-14, six DOF model. In the closed-loop configuration, the flight control laws receive rates and accelerations from the ISS DHS. The open-loop configuration was used to develop the DHS software; the closed-loop configuration was used to evaluate the DHS in a specific design situation.

Specific areas which were evaluated were failure threshold selection and related performance, DHS parameter sensitivity (i.e., cone angle alignment and c.g. location uncertainties), performance of the DHS with and without state estimator compensation and system performance in the presence of single and multiple induced sensor failures.

The digital simulation studies confirmed preliminary predictions relative to ISS performance. It was verified that the various types of single- and multiple-failure modes introduced in the gyros and accelerometers were detected and isolated by the DHS and this did not cause significant transients in control system performance. System sensitivity studies indicate that the DHS is tolerant to large misalignment (up to 0.2 deg) and large uncertainties in the lever arm between the sensor and c.g. ($\pm 15\%$).

The effectiveness of the state estimator in stabilizing the overall control system was also demonstrated. This is illustrated in Fig. 5, which shows the roll rate output from the ISS DHS superimposed on the roll rate generated in the six DOF model. The lower plot reflects the control system with the estimator bypassed. Here, oscillations feed through the flight control laws to the control surfaces, resulting in an erratic and oscillatory aircraft roll rate. The ability of the state estimator to normalize aircraft rates is shown in Fig. 6. The upper plot shows the aircraft roll rate during a level turn maneuver. The middle plot is the fuselage bending rate resulting from control system inputs. The lower plot is the residual roll bending after the DHS normalization. As can be seen by the scale change between plots, the DHS provides a high degree of compensation.

Laboratory Demonstration

Simulation Configuration

Figure 7 is a block diagram of the ISS laboratory demonstration configuration. A comparison with the representation of the digital simulation in Fig. 4 shows the same basic elements, i.e., ISS DHS, F-14 model, and skewed sensor data. In the laboratory simulation these elements were implemented using the following hardware and laboratory equipment:

1) Six skewed gyros (Honeywell GG445) and six skewed accelerometers (Honeywell GG326).

2) Three DOF flight attitude table (shown in Fig. 8) on which were mounted the cantilevered, simulated bulkhead, skewed sensors, and a three-axis rate and acceleration orthogonal reference package.

3) Perkin Elmer digital computer for executing a FORTRAN version of the airborne software, i.e., ISS DHS and flight control laws.

4) Analog computer for simulating the F-14 aircraft.

5) Interface electronics consisting of a combination of specially designed I/O devices and a general purpose 1 MHz data bus system.

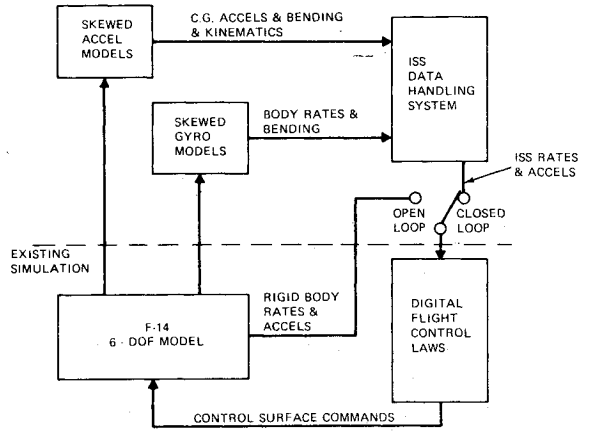

Fig. 4 Schematic representation of F-14/ISS digital simulation.

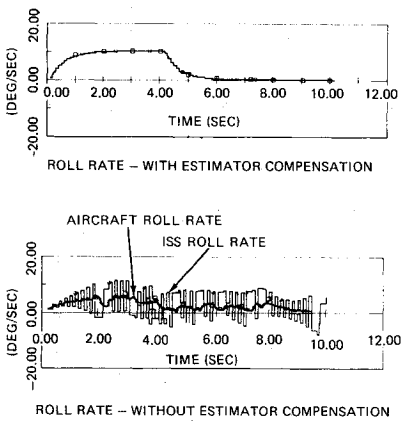

Fig. 5 Level turn maneuver, digital simulation.

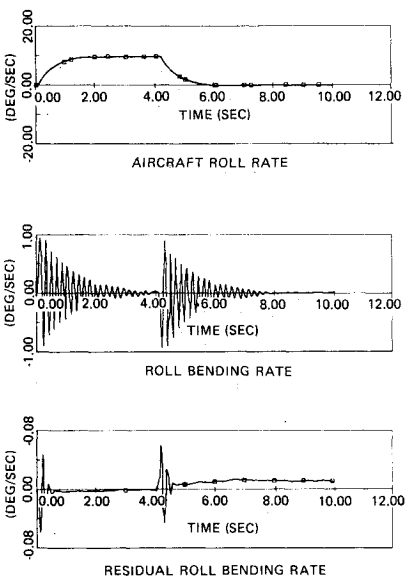

Fig. 6 Level turn roll rates, digital simulation.

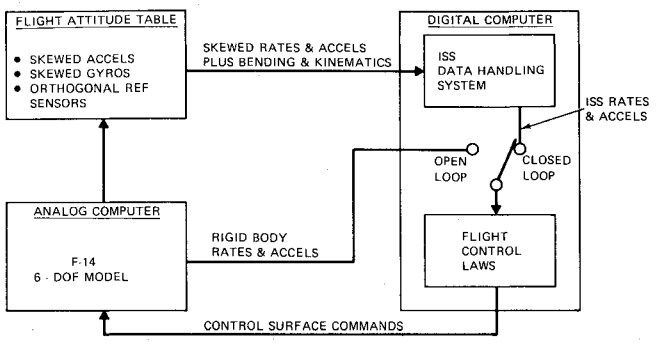

Fig. 7 Schematic representation of the ISS II laboratory demonstration configuration.

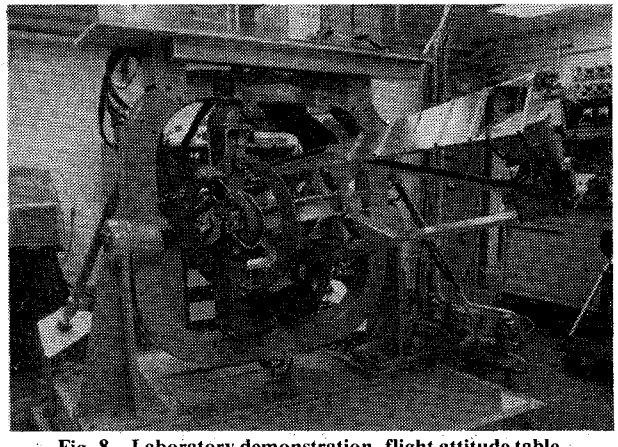

Fig. 8 Laboratory demonstration, flight attitude table.

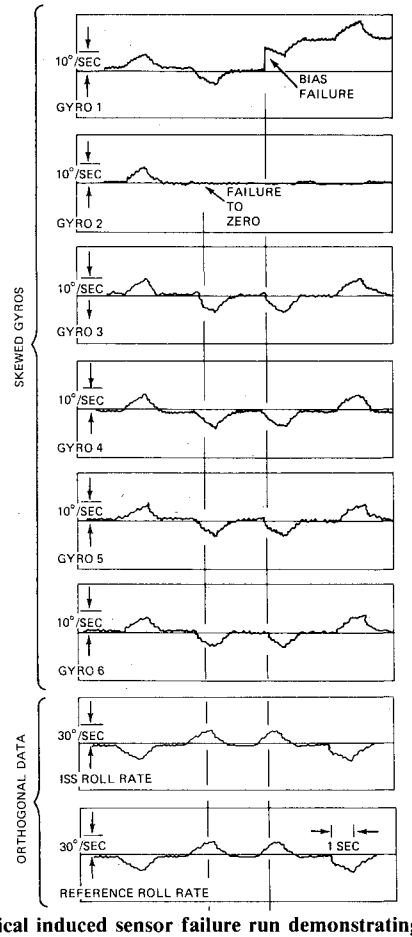

Fig. 9 Typical induced sensor failure run demonstrating continuity of ISS roll rate and reference roll rate during induced gyro failures.

Laboratory Testing Philosophy

To demonstrate the effectiveness of the normalization scheme in removing bending rates from the gyro data, the flight attitude table gimbal position commands were derived from the aircraft body rates plus the bending rates. Thus, the gyros mounted on the simulated bulkhead sensed the same total rates that would be experienced on the aircraft. The linear accelerometers, however, can sense only those accelerations caused by motions of the 4 ft cantilever mounting of the simulated bulkhead and the 1 g Earth field.

The cantilever fixture was designed to be essentially rigid, therefore, the sensed acceleration was computed to be,

$$a_k = \dot{\omega}_T \times h + \omega_T \times (\omega_T \times h) \tag{15}$$

where ω_T and $\dot{\omega}_T$ are the total angular rates and accelerations (including bending) respectively and h is the lever arm.

The state estimator was used to develop an estimate of these accelerations which is then subtracted from the total sensed accelerations. With the lever arm accelerations removed, the accelerations from the bulkhead mounted accelerometers were compared to the reference accelerometers, which were mounted at the center of the table.

Laboratory Test Objectives and Results

The laboratory test program included open- and closed-loop testing similar to the evaluation testing performed on the all-digital simulation. As before, laboratory testing emphasis was on verifying state estimator performance, verifying failure isolation capability, and monitoring aircraft performance in the presence of induced sensor failures. The significant results obtained from laboratory testing are that the state estimator design, modified for the laboratory test fixture, was effective in removing bending rates and kinematic accelerations; and that first and second failures of gyros and accelerometers were isolated with no observable transients in aircraft parameters. Results of a typical test run with two induced sensor failures is shown in Fig. 9 which presents the six skewed gyro signals, the roll rate derived by the ISS DHS, and the roll rate from the reference package.

Conclusions

The digital simulation and follow-up laboratory evaluation of the ISS lead to the conclusions that the skewed inertial sensor concepts, which utilize six rate gyros and six accelerometers, can provide dual fail-operational rate and acceleration data for digital fly-by-wire flight control systems as well as other aircraft subsystems. It was also found that implementation of this concept is feasible and practical for flight control applications using current digital computer technology to perform skewed inertial sensor redundancy management, including compensation for aircraft bending modes and kinematic acceleration effects. Finally, a state estimation scheme for performing the compensations for bending modes and kinematic accelerations was developed. This estimator, which was found necessary for system stability, also permits complete flexibility of sensor location for improved survivability and accessibility. It is to be noted that the state estimator design discussed in this paper was developed for flight control system applications. Simplifications and assumption used in the estimator design may have to be reconsidered in order to apply this DHS for navigation applications.

Acknowledgments

This work was funded by the Naval Air Development Center, Warminster, Pa. under Contract N62269-C-0206. Contract monitor was C. Abrams.

References

[1] Weinstein, W., "Feasibility and Design Studies of an Integrated Sensory Subsystem (ISS) for Advanced V/STOL Aircraft," Grumman Aerospace Corp., Rept. NADC 76259, March 1978.

[2] Abrams, C.R., Steele, R., and Weinstein, W.D., "An Integrated Sensory Subsystem (ISS) for Advanced V/STOL Aircraft," Paper presented at 3rd Digital Avionics Conference, Ft. Worth, Tx., Nov. 1979.

[3] Solomon, R., "Development of an Advanced Skewed Sensory Electronic Triad (ASSET) System for Flight Control," Grumman Aerospace Corp., Rept. NADC 77043-30, June 1979.

[4] Abrams, C.R., Solomon, R., and Weinstein, W.D., "Navy Advanced Sensor Programs for Fly-By-Wire Aircraft," *Proceedings of the AIAA, IEEE 2nd Digital Avionics Conference,* Boston, Mass., Nov. 1977.

[5] Weinstein, W., "Development of An Advanced Skewed Sensory Electronic Triad (ASSET) System for Flight Control," Grumman Aerospace Corp., Rept. NADC 76295-30, Oct. 1976.

[6] Kwakernaak, M. and Sivan, R., *Linear Optimal Control Systems,* John Wiley & Sons, New York, 1972, pp. 339-373.

[7] Berman, H. and Boudreau, J.A., "Dispersed Fly-By-Wire Sensor System for Improved Combat Survivability," *Journal of Guidance and Control,* Vol. 2, Nov.-Dec. 1979, pp. 463-470.